

HIGH-EFFICIENCY, DEEP-JUNCTION, EPITAXIAL InP SOLAR CELLS ON (100) AND (111)B InP SUBSTRATES

R. Venkatasubramanian, M.L. Timmons, and J.A. Hutchby
Research Triangle Institute
Research Triangle Park, North Carolina

and

R. Walters and G. Summers
U.S. Naval Research Laboratory
Washington, DC

ABSTRACT

We report on the development and performance of deep-junction ($\sim 0.25 \mu\text{m}$), graded-emitter-doped, n^+ -p InP solar cells grown by metallorganic chemical vapor deposition (MOCVD). A novel, diffusion-transport process for obtaining lightly-doped p-type base regions of the solar cell is described. The I-V data and external quantum-efficiency response of these cells are presented. The best active-area AM0 efficiency for these deep-junction cells on (100)-oriented InP substrates is 16.8%, with a J_{SC} of 31.8 mA/cm^2 , a V_{OC} of 0.843 V, and a fill-factor of 0.85. By comparison, the best cell efficiency on the (111)B-oriented InP substrates was 15.0%. These efficiency values for deep-junction cells are encouraging and compare favourably with performance of thin-emitter ($0.03 \mu\text{m}$) epitaxial cells as well as that of deep-emitter diffused cells. The cell performance and breakdown voltage characteristics of a batch of 20 cells on each of the orientation are presented, indicating the superior breakdown voltage properties and other characteristics of InP cells on the (111)B orientation. Spectral response, dark I-V data, and photoluminescence (PL) measurements on the InP cells are presented with an analysis on the variation in J_{SC} and V_{OC} of the cells. It is observed, under open-circuit conditions, that lower- V_{OC} cells exhibit higher band-edge PL intensity for both the (100) and (111)B orientations. This anomalous behaviour suggests that radiative recombination in the heavily-doped n^+ -InP emitter may be detrimental to achieving higher V_{OC} in n^+ -p InP solar cells.

INTRODUCTION

Epitaxial n^+ -p InP solar cells remain attractive for space photovoltaic applications as they have demonstrated a high AM0 conversion efficiency (~ 18 to 19%) [1]. These cell efficiencies have been obtained through material improvements by epitaxy as well as the use of a thin emitter ($\sim 0.03 \mu\text{m}$). However, the absence of photon-assisted annealing of radiation-induced defects and the consequent lack of superior radiation resistance of these epitaxial thin-emitter cells stand in sharp contrast to that observed in diffused, deep-junction ($\sim 0.3 \mu\text{m}$) cells [2].

This work aims to develop high-efficiency InP solar cells by MOCVD that replicate the diffused-junction structure, especially the deeper junction and the emitter surface doping gradient. The radiation resistance data from these cells are reported separately in a companion paper [3]. The goal is to improve the understanding of the radiation resistance of InP solar cells. In this work, we also present the first reported performance of InP solar cells on (111)B-oriented substrates.

The motivation for the study of cell performance on (111) orientation stems from the predicted advantages for hetero-epitaxial InP solar cells on Si substrates. There is about 8% lattice mismatch between InP and Si. This lattice mismatch can potentially introduce about $1.9 \times$

10^{14} dangling bonds per cm^2 at the interface of (100) InP-Si. However, the calculated dangling bond density for the (111) orientation is about 1.1×10^{14} per cm^2 . Thus, for similar growth conditions and defect control mechanisms, the (111) orientation potentially offers a 40% reduction in defect-density.

OMVPE GROWTH AND CELL STRUCTURE

The n^+ -p cell structures were grown on p-type InP substrates, doped to mid 10^{18} cm^{-3} . Fig. 1 shows the schematic of the cell structure. The best results of epitaxial growth on (100)-oriented substrates were obtained with use of no additional surface preparation to the customer-provided epi-ready InP wafers. However, it was found necessary to give a brief surface clean (consisting of a 1 min. etch in 1:1:5= $\text{H}_2\text{O}:\text{H}_2\text{O}_2:\text{H}_2\text{SO}_4$ solution followed by a thorough rinse in deionized water) for the (111)B-orientation substrates prior to epitaxy. This cleaning step is critical to obtaining a smooth epitaxy of InP layers on the (111) oriented substrates. The growth was carried out in an atmospheric-pressure MOCVD system using ethyldimethylindium and phosphine as the Group III and Group V precursors, respectively. All the growths were carried out at 700°C , with typical growth rates of $0.05 \mu\text{m}/\text{min}$.

Diethylzinc (DEZn) bubbler source was used for obtaining Zn-doping. An important requirement for obtaining high-efficiency as well as radiation-resistant n^+ -p InP cells is that the base region be lightly-doped to mid 10^{16} cm^{-3} . This lightly-doped base also enables the evaluation of a larger portion of the quasi-neutral p-base by techniques such as deep level transient spectroscopy (by applying a larger voltage-bias without breakdown of the junction) to study radiation-induced defects.

Typically, a low concentration dimethylzinc-in-hydrogen gas source is used for obtaining lightly-doped p-base. At RTI and other laboratories [4], this gas source has been found to lead to very erratic doping levels. Hence, in this work, we have investigated a new approach to obtain lightly-doped p-InP using a diffusion transport process. In this technique, the inlet of an organometallic-Zn bubbler is closed and the outlet is kept open. H_2 gas flow is maintained through a bypass line, adjacent to the bubbler, to continuously carry the organometallic-Zn that diffuses out from the bubbler to the growth zone.

This approach avoids the possible residual moisture and oxygen contamination, frequently present in gas cylinders, that can scavenge the Zn, especially at low ppm levels. Also, this approach is likely to provide a constant molar ratio of organometallic-Zn to H_2 , as long as the organometallic Zn-source is kept at a constant temperature, unlike a high-pressure gas-mixture that can lead to inconsistent concentration levels over the lifetime of the source.

We show in Fig.2(a) the polaron profile of a Zn-doped base region, obtained with a flow of 1ccm through a diethylzinc (DEZn) bubbler causing a carrier concentration of $\sim 4 \times 10^{18} \text{ cm}^{-3}$, suggesting ultra-low flow rates to get a p-doping level in mid- 10^{16} cm^{-3} . In Fig. 2(b), we indicate that with a 10ccm H_2 flow and using the diffusion-transport process, and using the vapor pressure of dimethylzinc (DMZn), we obtain a doping level of $\sim 6 \times 10^{17} \text{ cm}^{-3}$. In Fig. 2(c), we indicate that with the same 10 ccm H_2 flow and using the diffusion-transport process with a DEZn bubbler, we obtain a doping level of $\sim 8 \times 10^{16} \text{ cm}^{-3}$. The lower doping level obtained with the DEZn source is consistent with the lower vapor pressure of DEZn, compared to DMZn, therefore leading to a lower concentration of Zn although the same 10ccm of H_2 is used to transport the diffused species.

H₂Se gas source was used for obtaining the heavily doped n⁺ emitter regions. Se is the same Group-VI n-type dopant as in S-doped InP diffused junctions, as opposed to the use of Si in some of the work [1] of epitaxial InP cells. The emitter was nominally linearly graded with increasing H₂Se flow rates, to obtain a surface doping of $\sim 3 \times 10^{18} \text{ cm}^{-3}$.

The cell structure in Fig. 1 also indicates the use of Ti/Au (30nm/300nm) contact for the p+ InP substrate. This contact was sintered at 415°C for one minute. The front emitter contact was a non-alloyed AuGe/Ni/Au (50nm/10nm/300nm) metallization. The InP cells on (100)-oriented substrates received a two-layer ZnS/MgF₂ anti-reflection coating (ARC) as indicated in Fig. 1. The ZnS/MgF₂ coatings were deposited by e-beam evaporation. However, the cells on (111)B-orientation received a single-layer ARC of plasma-deposited silicon nitride because the e-beam evaporated ZnS/MgF₂ coatings strongly deteriorated the performance of the cells on (111)B-oriented substrates. The cause for this behaviour is not exactly clear at this point.

CELL I-V AND SPECTRAL-RESPONSE CHARACTERIZATION

The I-V and external quantum efficiency (spectral response) data of the cells were measured using an InP standard cell characterized at the National Renewable Energy Laboratory (NREL). Relative external quantum efficiency data for a deep-junction cell are shown in Fig. 3. The cell indicates a good red response and a small roll-off in the short-wavelength response. This roll-off is attributed to some recombination of photo-generated carriers either in the emitter region or at the surface of the emitter. The surface recombination velocity of n⁺InP has been predicted to be low [5]. In addition, the electric field resulting from the graded doping in the emitter is expected to oppose the surface recombination of minority carriers (holes) and accelerate them towards the depletion layer. As discussed below, based on photoluminescence data, we believe that the roll-off is related to radiative recombination of minority carriers in the heavily-doped n⁺-emitter regions. The radiative recombination is attributed to lower radiative-lifetimes in the quasi-neutral regions of n⁺-InP.

The best active-area AM0 efficiency for these deep-junction cells on (100)-oriented InP substrates is 16.8%, with a J_{sc} of 31.8 mA/cm², a V_{oc} of 0.843 V, and a fill factor of 0.85. By comparison, the best cell efficiency on the (111)B-oriented InP substrates was 15.0%, with a J_{sc} of 31.3 mA/cm², a V_{oc} of 0.797 V and a fill factor of 0.815. These efficiency values for deep-junction cells are encouraging and compare favorably with performance of thin-emitter (0.03 μm) epitaxial cells as well as that of deep-emitter diffused cells.

The cell (efficiency) performance of a batch of ~20 cells, each on (100)- and (111)B-oriented InP substrates, are shown in Fig. 4. We can immediately observe the spread of cell efficiencies, for both the orientations, over a reasonably wide range. However, we note the tighter (and a more statistically expected Gaussian-like) spread of cell efficiencies on (111) substrates and a more random fluctuation on the (100) substrates.

ORIENTATION-EFFECTS ON REVERSE-BREAKDOWN VOLTAGES

Similar statistical behavior in the breakdown voltage of cells on (100) and (111)B substrates was obtained. Fig. 5 shows a histogram depicting the distribution of breakdown voltages of the cells on the two orientations. For a given base doping level, the breakdown voltages of nearly all the cells on (111) InP substrates were within 4.5-5.2 V, while the cells on (100) substrates had considerable variation. Two of the cells, from the same wafer of (100)

orientation, with very similar forward characteristics had completely different reverse-breakdown characteristics. In contrast, any two cells even from different wafers of (111) orientation had similar reverse characteristics.

The cause for this variance in behavior of reverse-breakdown characteristics is thought to be related to the more electronically-active (111)B InP surface than the (100) surface [6], leading to a more stabilized surface from a more-accelerated native-oxidation process. Thus the junctions on (111)-oriented substrates probably suffer from less surface-induced, soft-breakdown reverse-characteristics. In addition, it has been reported that under certain doping conditions, the (111) orientation can offer significantly higher breakdown voltages than the (100) orientation in GaAs [7].

In any case, the reproducibility of InP cell-efficiency and breakdown-voltage characteristics on (111)B-oriented substrates, compared to (100)-orientation, is noteworthy. This portends well for the investigation of InP cells on (111)-Si substrates.

PL CHARACTERIZATION OF InP CELLS

Band-edge photoluminescence (PL) from the InP cells were also evaluated at 300K to understand the variation in J_{sc} and V_{oc} of the cells. The PL excitation source was an Ar-ion laser operating at 515 nm. The PL measurements were conducted under open-circuit conditions and the laser radiation is expected to be fully absorbed within the 0.25- μm -deep emitter region.

In Fig. 6, we indicate the PL data from two InP cells on (100) substrates, nominally grown with the same cell structure (shown in Fig. 1) and nearly identical J_{sc} values. The cell (1-1955-a-4), with a significantly higher V_{oc} (0.843 V), shows a much smaller band edge PL signal than the cell (1-1961-a-4) with a lower V_{oc} of 0.783 V. The same pattern is once again observed in cells grown on the (111)B orientation, and is shown in Fig. 7, i.e., the lower V_{oc} cells indicate higher band edge PL intensity. This leads us to suggest that the lower V_{oc} of n^+ -p InP cells is perhaps related to lower radiative lifetime in the n^+ -emitter regions. This argument would be consistent with the higher PL intensity and the well-documented low surface-recombination velocity of n -InP and n^+ -InP surfaces.

It has been known for some time that the open-circuit voltage of state-of-the-art n^+ -p InP solar cells are not as high as that one would expect for its bandgap [1], in relation to that observed in GaAs, especially considering that the surface recombination velocity of native n^+ -InP surfaces are comparable to those at high-quality GaAs-AlGaAs interfaces in GaAs solar cells. This discrepancy has not been resolved [1]. We believe that the high n -type doping level (~high 10^{18} cm^{-3} to low 10^{19} cm^{-3}) used in these cells probably result in low radiative lifetimes, leading to lower-than-ideal V_{oc} of cells. A lower emitter doping, in conjunction with a thicker emitter (like 0.1 μm) to maintain low emitter sheet resistance, is worth an exploration. Recently at RTI, we have been able to improve the V_{oc} of the InP cells from above-mentioned 0.843 V to 0.875 V, one of the highest-reported values for InP cells under AM0 conditions, with the use of reduced doping levels in the emitter.

It may be worth pointing out that the J_{sc} levels in n^+ -p InP cells are less sensitive to any reduction in lifetime (from higher doping level) in the emitter-region as the combination of low surface recombination velocity of n^+ -InP and reasonable diffusion lengths can cause near-complete collection of photo-generated carriers from the emitter. This was evident in our deep-junction cells as well, where, the variation of V_{oc} was present in cells with very similar J_{sc} values. This effect was noticeable in both the orientations of InP substrates.

SUMMARY

In summary, we have developed and characterized the performance of deep-junction ($\sim 0.25 \mu\text{m}$), graded-emitter-doped, n^+ -p InP solar cells, grown by metallorganic chemical vapor deposition (MOCVD). A novel, diffusion-transport process for obtaining lightly-doped p-type base regions of the solar cell, was described. The best active-area AM0 efficiency for these deep-junction cells on (100)-oriented InP substrates is 16.8%, with a J_{SC} of 31.8 mA/cm^2 , a V_{OC} of 0.843 V, and a fill factor of 0.85. By comparison, the best cell efficiency on the (111)B-oriented InP substrates was 15.0%. The cell performance and breakdown voltage characteristics of a batch of 20 cells on each of the orientation were presented, indicating the superior breakdown voltage properties of InP cells on the (111)B orientation. Spectral response, dark I-V data, and photoluminescence (PL) measurements on the InP cells were presented with an analysis on the variation in V_{OC} of the cells. It is observed, under open-circuit conditions, that lower- V_{OC} cells exhibit higher band-edge PL intensity for both the (100) and (111)B orientations. This behaviour suggests that radiative recombination in the heavily-doped n^+ -InP emitter may be detrimental to achieving higher V_{OC} in n^+ -p InP solar cells.

REFERENCES

- 1) C.J. Keavney, V.E. Haven, and S.M. Vernon, Proc. of 21st IEEE Photovoltaic Specialists Conf., (IEEE, NY), 141 (1990).
- 2) M. Yamaguchi and K. Ando, J. Appl. Phys., 63, 5555 (1988).
- 3) R.J. Walters, G.P. Summers, M.L. Timmons, R. Venkatasubramanian, J.A. Hancock, and J.S. Hills, Paper Presented at this SPRAT Conference.
- 4) R. Venkatasubramanian and S.K. Ghandhi, Unpublished Results of work on low p-type doping of GaAs at Rensselaer Polytechnic Insitute, Troy, NY, 1983.
- 5) R. K. Ahrenkiel in *Properties of Indium Phosphide*, emis Datareviews Series No.6, INSPEC, p.80, 1991.
- 6) S.K. Ghandhi, *VLSI Fabrication Principles - Silicon and Gallium Arsenide*, John Wiley, NY, p.13, 1983.
- 7) M.H. Lee and S.M. Sze, Solid St. Electron. 23, 1007 (1980).

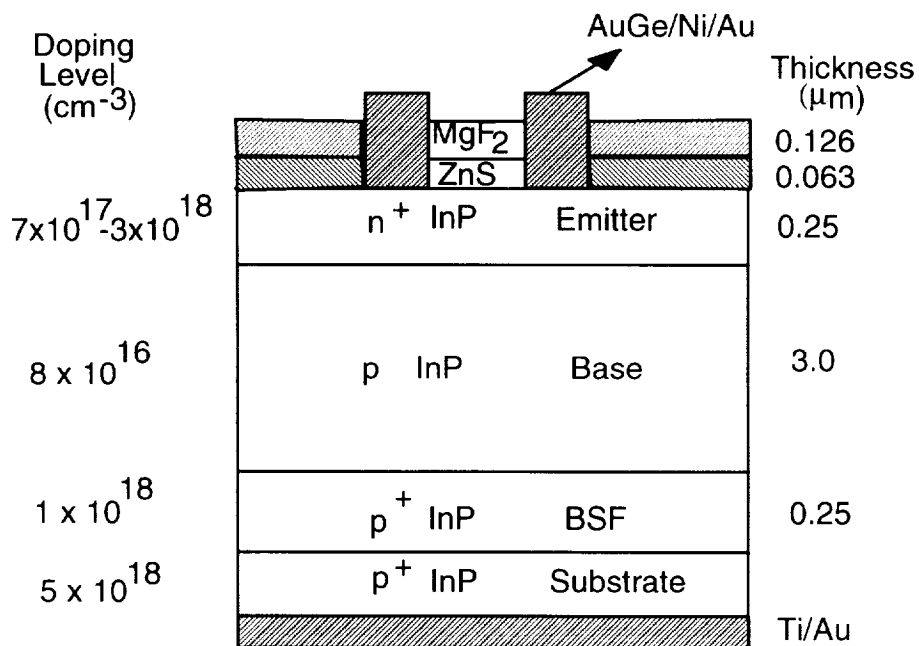


Fig. 1 Schematic of a n⁺-p InP solar cell structure indicating the graded emitter doping.

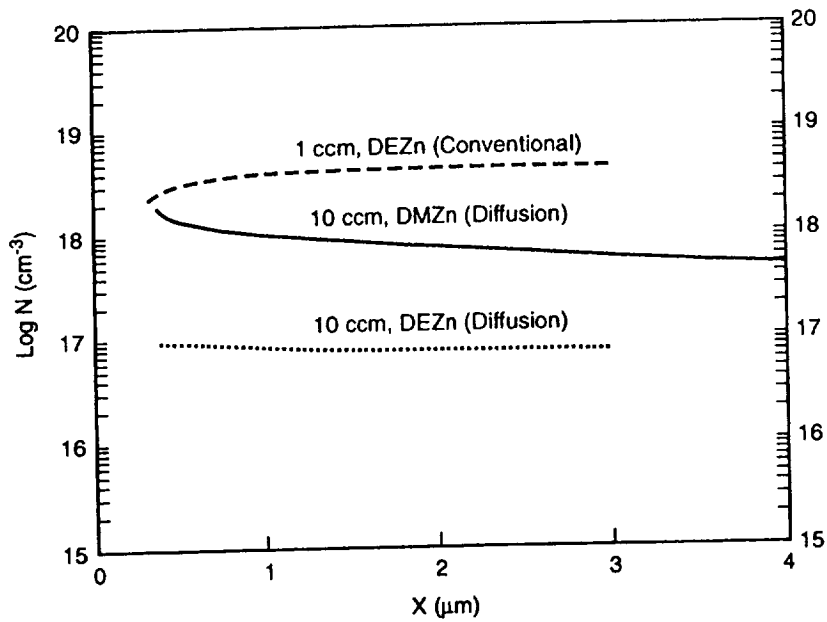


Fig. 2 Polaron doping profiles for (a) conventional Zn-doping with 1ccm H₂ bubbled through a DEZn bubbler, (b) diffusion-transport with 10ccm H₂ using the vapor pressure of DMZn and (c) diffusion-transport with 10ccm H₂ using the vapor pressure of DEZn.

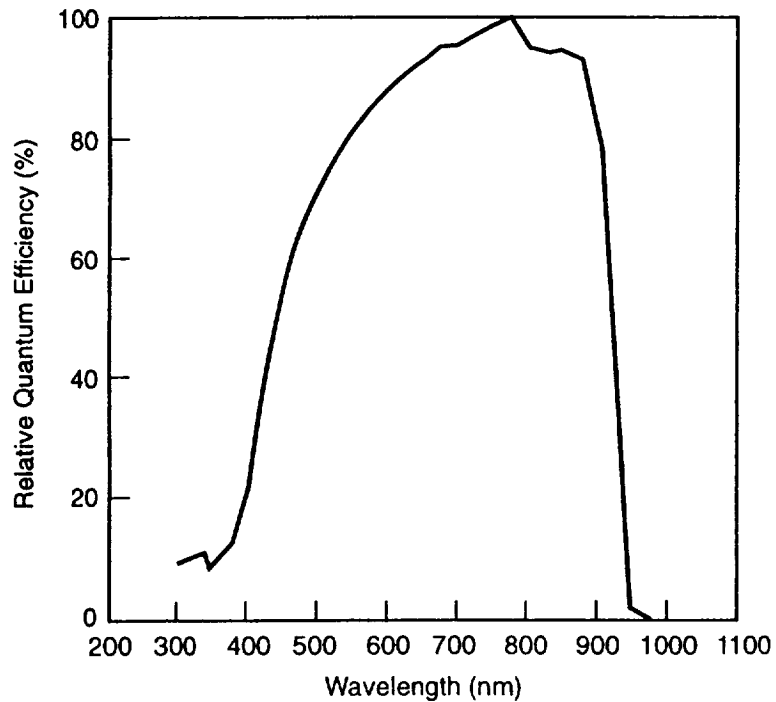


Fig. 3. External quantum efficiency of a deep-junction, n⁺-p InP cell measured at NREL.

**EFFICIENCY COMPARISON
ON <100> AND <111> SUBSTRATES**

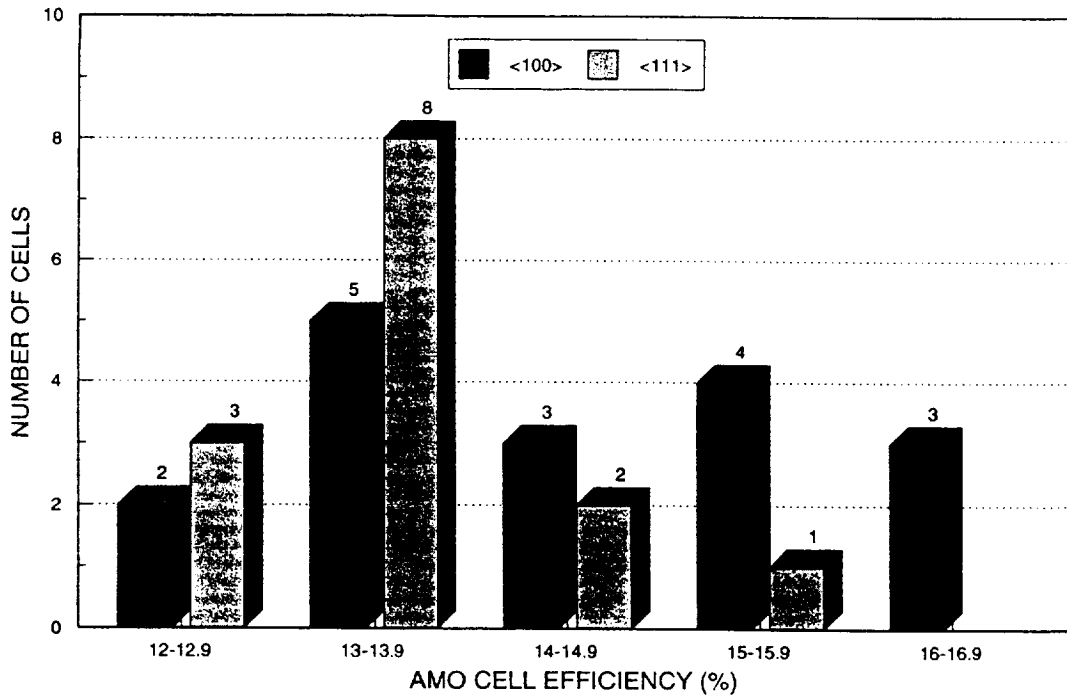


Fig. 4 Cell (efficiency) performance histograms for (100) and (111)-B InP substrate orientations.

**BREAKDOWN VOLTAGE COMPARISON
20 CELLS ON <100> AND <111>**

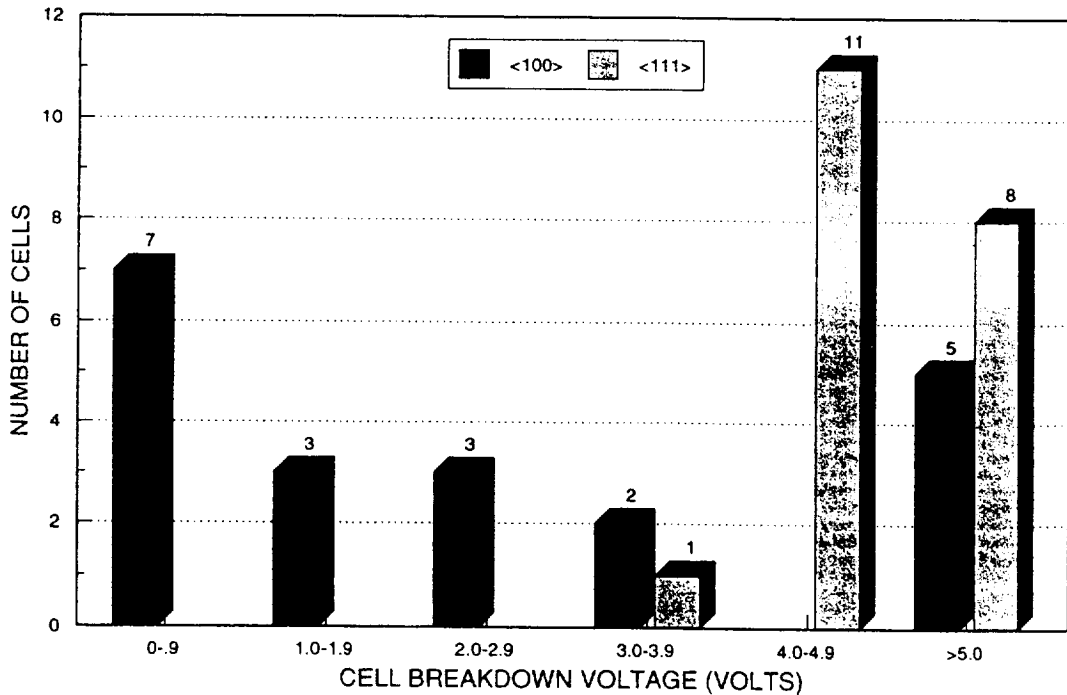


Fig. 5 Cell (reverse breakdown voltage) performance histograms for (100) and (111)-B InP substrate orientations.

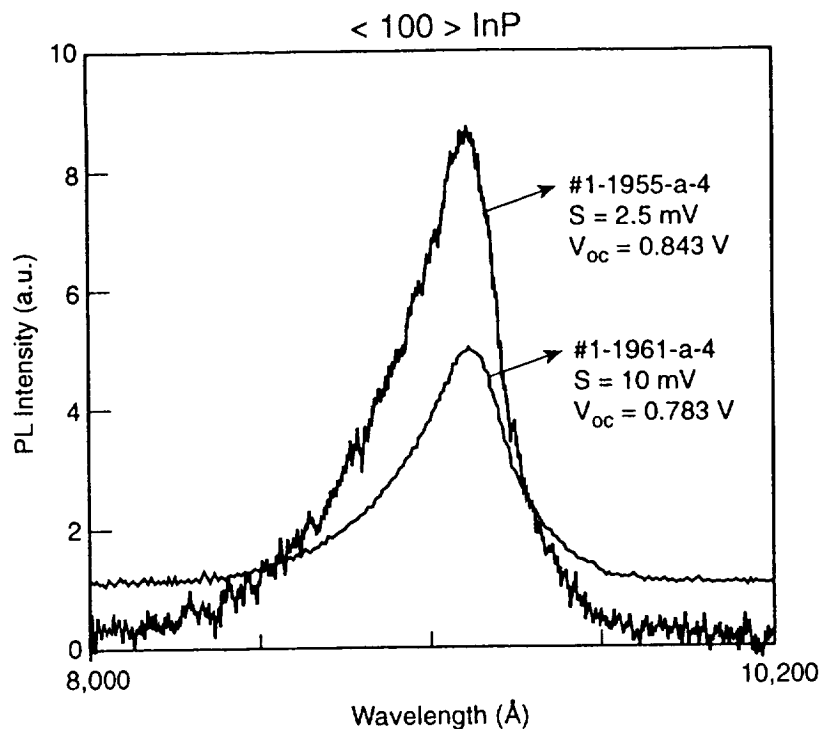


Fig. 6. 300K PL data (under open-circuit conditions) from two InP cells on (100)-oriented substrates, with nearly identical J_{SC} values, but different V_{OC} values.

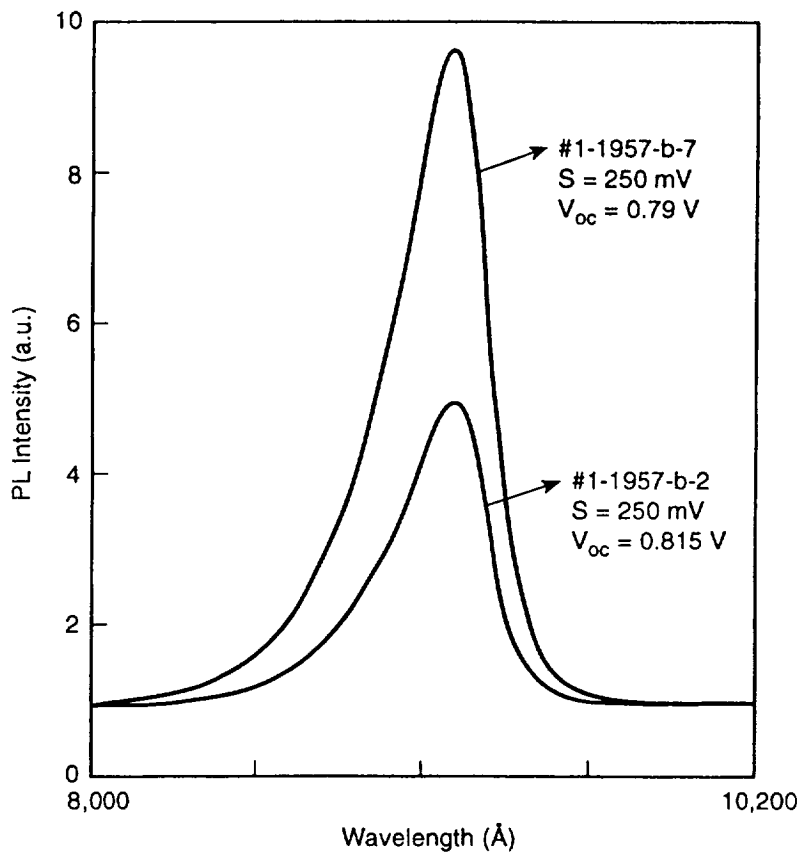


Fig. 7. 300K PL data (under open-circuit conditions) from two InP cells on (111)B-oriented substrates, with nearly identical J_{SC} values, but different V_{OC} values.

